ACS APPLIED MATERIALS & INTERFACES

Research Article

www.acsami.org

Tuning Gold Nanoparticles Interfaces by Specific Peptide Interaction for Surface Enhanced Raman Spectroscopy (SERS) and Separation Applications

Anastasios C. Manikas,[†] Filippo Causa,*[,†,‡,§] Raffaella Della Moglie,[†] and Paolo A. Netti[†,‡,§]

[†]Center for Advanced Biomaterials for Healthcare@CRIB, Istituto Italiano di Tecnologia (IIT), Largo Barsanti e Matteucci 53, 80125 Naples, Italy

[‡]Interdisciplinary Research Centre on Biomaterials (CRIB), University "Federico II", Piazzale Tecchio 80, 80125 Naples, Italy

[§]Dipartimento di Ingegneria chimica, dei Materiali e della Produzione industriale, University "Federico II", Piazzale Tecchio 80, 80125 Naples

Supporting Information

ABSTRACT: Surface functionalization and control over nanostructured interfaces represents a key aspect in nanoscience and nanobiotechnology. Nanoplasmonic structures for analyte detection typically require sophisticated nanofabrication techniques, as well as bioactivated nanostructures that need multistep conjugations for chemical ligation. An alternative to such complex processes is to rely on specific biomolecules adsorption for decoration or self-assembly of nanoparticles at solid/liquid interface. In principle, small biomolecules with specific binding properties to nanostructures could control the assembly without modifying the nanoparticle chemistry, pH of the solution or salt concentration. Importantly, such an approach could be direct, robust, and reversible. In this work, we report about the use of a specific peptide for direct and reversible adsorption on gold nanoparticles with tuned interfacial properties just by simply adjusting the ratio between the numbers of peptide molecules to the number of gold nanoparticles. This easy, direct and reversible assembly of gold nanoparticles mediated by the specific peptide makes this platform ideal for small-volume samples and low concentrations detection using surface enhanced Raman Spectroscopy, as well as for the capture or separation of biomolecules in complex mix

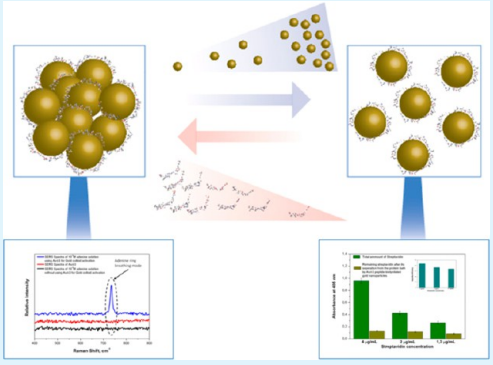

KEYWORDS: *peptides, gold nanoparticles, adsorption, assembly, SERS*

INTRODUCTION

Metal nanoparticles have attracted a great deal of attention because of their unique optical electronic properties and potential applications in biological, optoelectronic, and photonic technology.[1−3] In particular, the interaction of metal nanoparticles with optical fields results in collective oscillations of conduction electrons within the nanoparticles, known as plasmon resonance. The plasmon resonance energy of metal nanoparticles depends on several factors, such as the size and shape of the particles, the dielectric environment for isolated nanoparticles and the interactions between the particles in aggregated structures. More specific, gold nanoparticles possess specific physical and chemical attributes that make them excellent scaffolds for the fabrication of novel chemical and biological sensors.[3−11] Gold nanoparticles can be synthesized in an unambiguous way with highly stable and unique optoelectronic properties. They can also provide high surface-to-volume ratio with excellent biocompatibility by using appropriate ligands. These properties can be ad hoc tuned by varying their size, shape, and the surrounding chemical environment. In addition, gold nanoparticles offer a suitable platform for multifunctionalization with a wide range of organic or biological ligands for the selective binding and detection of small molecules and biological targets.[5−7,10]

All these unique properties of metal nanoparticles give an increasing interest in the preparation of nanoparticles that are stable in aqueous media and can be readily functionalized with biomolecules by established bioconjugation procedures. Such materials can be used for many applications including biolabeling for a range of optical and electron microscopic techniques, biosensing and as potential carriers for drug and gene delivery.[12−14] Gold nanoparticles, have been investigated extensively in this context owing to their excellent stability and relative ease of preparation.[16] Several efficient stabilization methods based on capping the particles with protective thiol-based ligands have been reported, including the use of mercaptodextranes,[17] thiolated PEG derivatives,[18−24] and peptides.[25−35] A number of different approaches to conjugating such particles to biomolecules have also been reported. These include click chemistry,[36] biotin−avidin coupling,[37−39] ligand

Received: May 24, 2013
Accepted: July 17, 2013
Published: July 17, 2013

exchange,[40,41] and a range of standard bioconjugation procedures.[42,43]

On the other hand, peptides undergo distinctive sequence-specific self-assembly[44] and have recognition properties,[45,46] thus making them important structural and signaling molecules in biological systems. The inclusion of specific peptide sequences with unique biological properties resulted in a large number of biocompatible biomaterials being self-assembled by using peptide conjugates as building blocks.[47,48] These biomaterials exhibit a variety of promising applications such as drug delivery,[49] regenerative medicine,[50,51] and hemostatic agents.[52] Such attributes, namely, the self-assembly and recognition capacities of peptides, are useful as building blocks for directing the growth and assembly of inorganic nanostructures. Various molecules can be attached to peptides to affect their self-assembly properties and direct their assembly into particular desired structures. Such modified peptides are often named "peptide conjugates". Peptide conjugates can self-assemble into various well-defined nanostructures, such as micelles, vesicles, nanotubes, and nanoribbons, through ionic and hydrophobic/hydrophilic interactions, including p−p stacking and hydrogen bonding.

Recently, peptides have been introduced as binding ligands to metal nanoparticles.[53] In the specific issue of inorganic binding peptides,[54,55] the selected sequences exhibited the ability to control the synthesis of relevant technological materials.[56,57] This led to the possibility to employ the peptides binding ability to create molecular linkers and thus control agents and to create innovative hybrid systems (organic/inorganic) for nanobiological applications.[58] To this regards we have already selected a dodecapeptide for specific binding on gold via hydrophobic interactions.[61] Other peptide functionalized gold nanoparticles were both single gold nanoparticles decorated with peptides and big gold aggregates[59] around 500 nm. Usually peptide binds on gold surface via covalent Au−S interactions[26] but there are also non covalent binding[60] reported. The covalent interactions form stable functionalized nanoparticles with a lack of size tuning due to the strength and the nature of Au−S binding. Size tuning have been reported and achieved by pH changes.[27] Such tuning should be observed with environmental changes, fact that prevents the in vivo applications capability of the material. Another crucial characteristic for functionalized gold nanoparticles, which gives them a bigger spectrum of applications is the reversibility of the assembly/disassembly process and the preferable shifting from single decorated gold nanoparticles to big aggregates of gold. In the literature, this has been reported by N-IR illumination that results in a disassembly to thermally responsive plasmonic nanoparticles with thermally labile biomolecular linkers[26] but also pH changes.[15] So, reversible self-assembly of peptide-functionalized gold nanoparticles have been only achieved by adjusting external environmental parameters (pH, illumination, linkers...). On the other side, control and reversible assemblies of gold nanoparticles has been recently demonstrated by the modulation of hydrophobic interactions through solvent change.[62]

Here we report for the first time a direct and simple use of an AuΦ3 peptide for the functionalization of gold nanoparticles in a controlled and reversible way via hydrophobic interactions. In particular, reversible self-assemblies of functionalized gold nanoparticles just by adjusting the ratio of Number of peptide molecules to Number of gold nanoparticles without the change of any other parameters (pH, temperature, chemicals, solvents), single decorated gold nanoparticles to submicrometer aggregates have been created. These assemblies have been extensively characterized, using different experimental techniques, such as UV−vis absorption spectroscopy and TEM microscopy, and the mechanism of this assembly and disassembly process have been described. Finally, two representative applications, one about gold aggregates and one about single decorated gold nanoparticles, are presented to show the broad function range for this new material. On the one hand, peptide mediated gold aggregated particles were used for generation of SERS active substrates; on the other, single decorated gold nanoparticles were used for streptavidin separation from a protein bath.

EXPERIMENTAL SECTION

Au gold nanoparticles 20 nm were purchased from BBInternational. AuΦ3 peptide (TLLVIRGLPGAC) was synthesized as analytically described[61] and stored at −20 °C until use. After synthesis, peptides were added in gold nanoparticles solution to a final ratio presented in Supporting Information Table 1 and incubated in room temperature to provide a peptide-gold nanoparticle conjugates. Peptide modified with FITC and Biotin has been also synthesized with a similar procedure by adding such moieties to the N-terminal of AuΦ3 peptide. Streptavidin-conjugated alkaline phosphatase, p-nitrophenyl phosphate which was used for the Elisa tests and BSA (bovine serum albumin) was purchased from Sigma Aldrich.

UV−vis absorption spectroscopic measurements were performed on peptide−gold nanoparticles conjugates solutions placed in 1 cm path-length quartz optical cuvettes. Spectra were recorded with a Cary 100 UV−vis spectrometer from 200 to 800. The estimated resolution was 1 nm and background was corrected with Milli Q water.

Electron microscopy samples were prepared on a 200 mesh fromvar copper TEM grids from Agar scientific. One drop of solution was applied to the grid from a pipet. After solution evaporation the grid was washed with deionized water to remove salt excess from grid surface. Scanning transmission electron microscopy was performed with a Cryo-TEM tomography TECHNAI 20 FEI COMPANY. The images were acquired on a vacuum generator operated at 250 kV with camera (FEI-EAGLE) exposure time of 1 s. The estimated point to point resolution was 2 A.

For fluorescence acquisitions, samples were added in 3520-050 borosilicate rectangle capillary tubing by VITROTUBES and placed under the microscope. For the focusing of the laser and the collection of the scattered light a 25×/0.95 water immersion objective were used. The system was excited with an argon$^+$ laser at 488 nm and the emission bandwidth was from 500 to 550 nm. Fluorescence spectra were recorder with a Leica confocal microscope SP5 from Leica Microsystems.

The Raman spectra were excited with a diode laser 780 nm. An 10×/×0.25 objective was utilized to focus the laser beam into the well plate which were filled with gold nanocolloidal suspensions. The Raman spectra were acquired with a DXR Raman spectrometer from Thermofischer Scientific with 20 mW laser power.

RESULTS AND DISCUSSION

As it clearly has been described above, the formation of decorated gold nanoparticles which can be tuned from single particle to gold aggregates (with a parallel preferable shifting to its plasmonic characteristics) without any external environmental changes like pH and temperature would be favorable with a broad spectrum of applications. Here, 20 nm gold nanoparticles have been functionalized with the AuΦ3 peptide, which has the potential to form reversible gold nanomodes as described, from single particle to gold aggregates and vice versa just by adjusting the molecular ratio (number of peptide to number of gold nanoparticles).

More specific, 200 μL peptide solution 16.8 μg/mL were added in 500 μL gold nanoparticles to a final ratio 5000. Ongoing, 10 μL of sample 1 added in 630 μL of gold nanoparticles to a final ratio 80, and final 200 μL of the same peptide solution added in to the sample 2 to a final ratio again around 5000. UV−vis absorption spectra of these samples were recorded and presented in Figure 1. The observed spectroscopic changes with the respective TEM images in each one of the steps proved this reversibility of the procedure. This reversibility gives to this material the advantage by adjusting the ratio of peptide to gold nanoparticles to tune the gold nanoparticles formation (from single decorated to big aggregates) and the material characteristics. This reversible self-assembly of gold nanoparticles broadens the spectrum of this material's applications, which can be regulated also on real time experimental conditions.

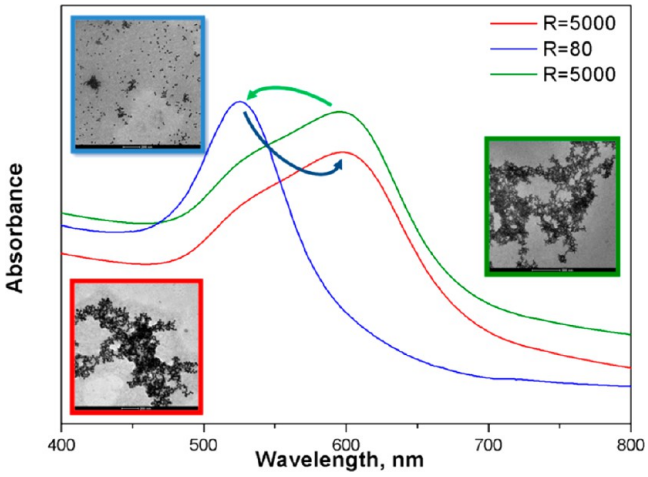

Figure 1. UV−vis absorption spectra of peptide functionalized gold nanoparticles, in the beginning the sample was with high peptide loading (R = 5000) then was driven to very low peptide loading (R = 80) and then again to the starting state (R = 5000).

In order to understand and to explain the behavior of the functionalized gold nanoparticles with the AuΦ3 peptide, a deep characterization of the starting materials but also of the created modes was necessary. ζ-Potential measurements and fluorescence microspectroscopy were employed for the verification and the quantification of the amount of the adsorbed AuΦ3 peptide on the gold nanoparticles in all the different molecular ratios. Transmission electron microscopy (TEM) images were recorded for the optical characterization of the formed modes and UV−vis absorption spectroscopy was necessary to show as photophysical changes of the material in the different molecular ratios.

Photophysical and optical characterizations of the starting materials (peptides and gold NPs) were performed by using UV−vis absorption spectroscopy and TEM. Gold nanoparticles have shown strong and continuous absorption spectrum (Figure S1 Supporting Information) with a maximum at around 520 nm. The size has been determined with DLS measurements and found around 18 nm. This result has been also verified by TEM (Figure S1 Supporting Information). On the other hand, it is also crucial to have a slight photo physical characterization for the peptide itself. UV−vis absorption spectra of peptide solution (Figure S1 Supporting Information) showed continuous absorption spectrum with a maximum at around 270 nm, far away from the specific band of gold nanoparticles.

It was of great importance to find a way to study the gold nanoparticles surface and possible charge changes because of peptide adsorption. For this reason ζ-potential measurments were performed in the reported gold nanoparticles to peptide molecules ratios. It is clearly shown in Figure 2 that there is an

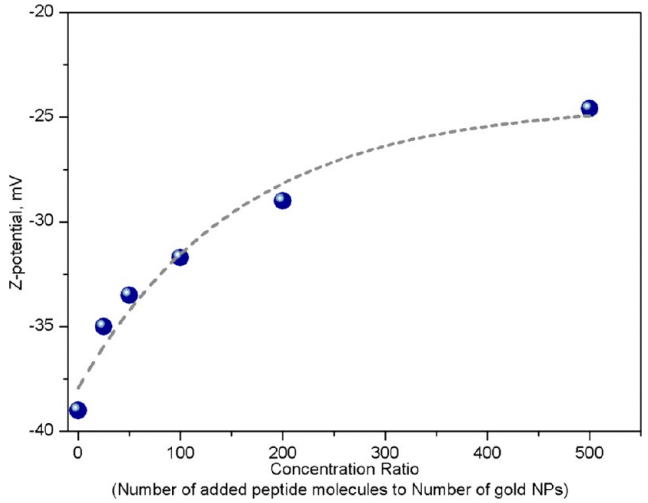

Figure 2. ζ-Potential measurments of gold nanoparticles upon the addition of AuΦ3 peptide.

increase on the ζ-potential because of the peptide addition. More detailed, the ζ-potential of the net gold nanoparticles is around −40 mV and this value increases to −25 mV upon AuΦ3 addition for R = 500. The positive peptide (+1 which have been Calculated by subtracting the number of basic residues R and K from the number acids residue D and E) when adsorbed on the gold nanoparticles surface contributes to the total surface charge resulting an increase to the total surface charge as reported in Figure 2. The decreasing growth of ζ-potential until −25 mV can be also explained. At the beginning all of the gold nanoparticles on the outer surface are free so the peptides can be easily adsorbed, while this procedure goes on the adsorption on the surface and also the changes of the surface charge becomes lower because of limited available area. The plateau value corresponds to the total charge when the gold nanoparticles surface is fully occupied with AuΦ3 peptide.

UV−vis absorption spectroscopy has been used for the optical characterization of each sample. In specific, likely changes of UV−vis absorption spectrum of gold nanoparticles were examined in order to collect information about the peptides-gold nanoparticles interactions. Spectra collected from the peptide−gold nanoparticles conjugates are shown in Figure 3.

Significant changes to the absorption spectra because of the peptide addition on the gold nanoparticles solution occurred. More specific, for low ratios until R = 125, an increasing small red-shift of around 3−4 nm to the center of the absorption band appeared (as compared to the gold nanoparticles absorption spectra) and a small broadening of the absorption band to the higher wavelengths was observed. Moreover, at the higher ratios a new band appeared at around 605 nm whose intensity has been found to increase with R. This new band contributes also to the spectra of the low ratios even if this was not visible, which explains also the small shift and broadening

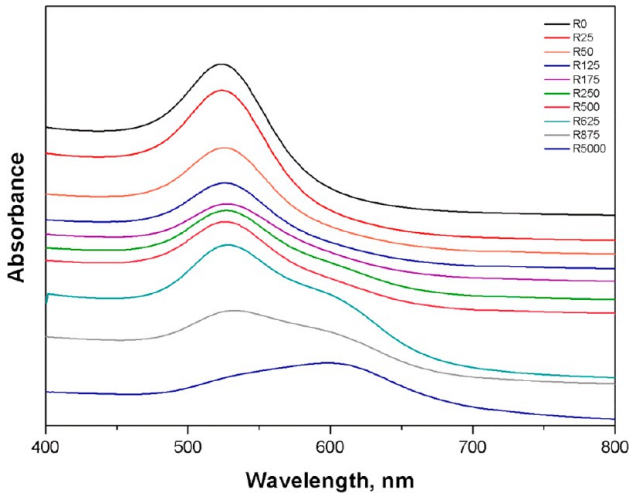

Figure 3. UV−vis absorption spectra of Au nanoparticles upon addition of different amounts of AuΦ3 peptide.

of the spectra at this ratios. These changes of the gold nanoparticles UV−vis absorption spectra can be attributed to a generated aggregation of nanoparticles due to the presence of the peptide. When the quantity of the peptide is small, the generated aggregations are small and a few with minor spectroscopic changes, but when the quantity of the peptides becomes bigger, the aggregated nanoparticles become larger with considerable spectroscopic changes. Theoretically, the physical nature of this surface plasmon mode, which gives colloidal Au its characteristic intense burgundy color, is well understood and has considerable dependence on particle size and shape. When the inter particle repulsive forces are sufficiently screened by peptide adsorption, aggregation occurs and generates a new red-shifted feature in the optical spectrum at around 600 nm. This aggregated band results from coupling of surface plasmons between closely spaced particles. In aggregated colloids, the particles are physically connected, but it is essential to note that direct contact is not always needed to observe collective plasmon modes. In fact, as long as the spacing between particles is small compared to the wavelength of light, these collective plasmon modes can be observed. UV−vis is particularly well-suited for analyzing this type of samples, as the optical spectra of Au colloid monolayers on transparent substrates is easily measured.

It was critical for the experimental procedure to verify with an unambiguous way the primary results came out from the study of UV−vis absorption spectra. Transmission electron microscopy (TEM) gave us the opportunity for a visual

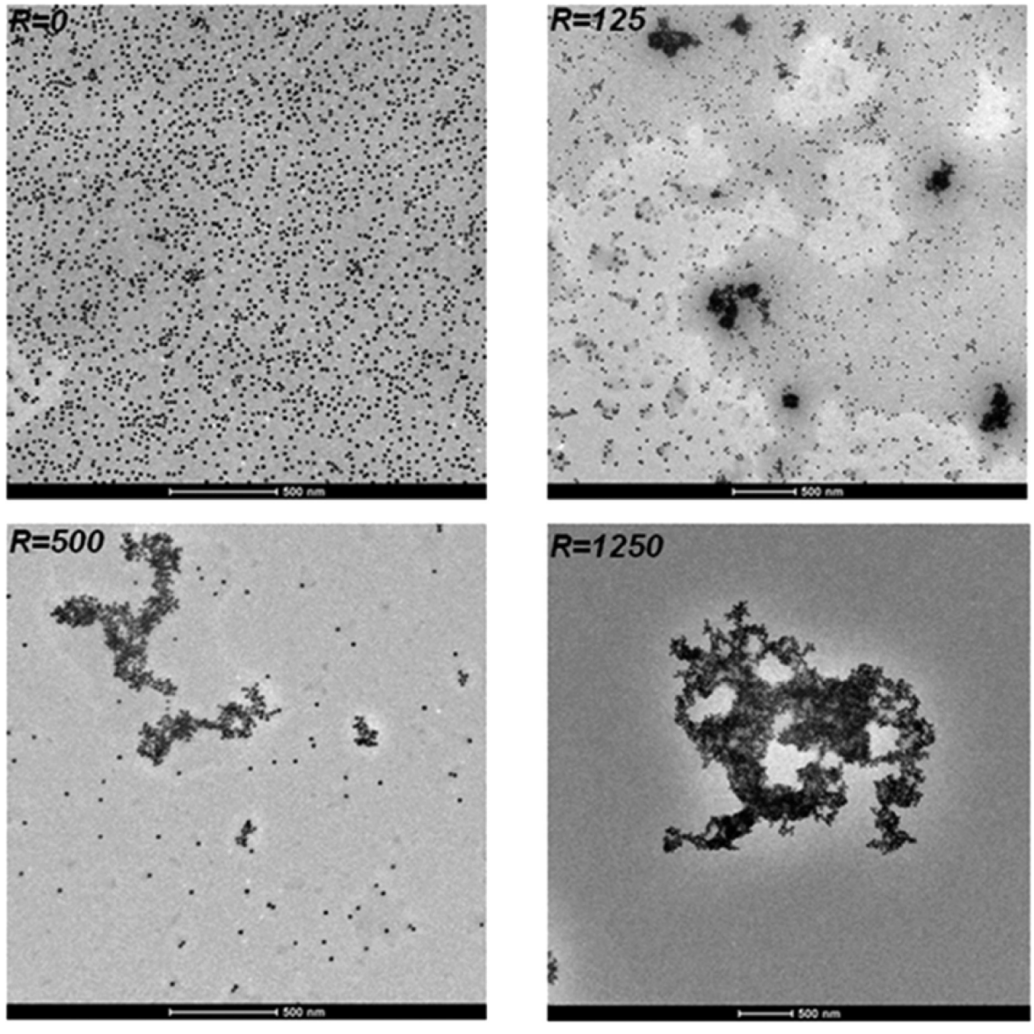

Figure 4. Transmission electron microscopy images of peptide functionalized gold nanoparticles at different ratios.

presentation of this phenomenon. TEM images of different samples are shown in Figure 4.

It is clearly demonstrated in Figure 4 that compared to the TEM image of net gold nanoparticles there is an aggregation because of the peptide concentration added on the gold nanoparticles. This aggregation found to be proportional to the peptide concentration. These results come in strong correlation to these from UV−vis spectroscopy in which we finally assumed an aggregation of the gold nanoparticles.

The aggregation of gold nanoparticles due to peptide adsorption was observed either with UV−vis absorption spectroscopy because of a red-shift and a broadening to the spectrum either with TEM microscopy. Nevertheless, the peptide concentration adsorbed on the gold nanoparticles was not possible to be determined with these techniques. FITC modified peptides were added to the gold nanoparticles in the same ratios and the quantity of adsorbed peptides on the gold nanoparticles surface was determined by using fluorescence microspectroscopy. The idea of employing FITC modified peptides was that using fluorescein, a strong fluorescence dye, the amount of peptide which adsorbed on gold nanoparticles surface can be detected and finally quantified. For the quantification, a calibration curve of the FITC modified peptide in solution with fluorescence spectroscopy was necessary to be created. Standard samples with known concentration were prepared and fluorescence spectra were recorded. Taking in account the intensity of fluorescence for each concentration of FITC-peptide, the calibration curve was formed (Supporting Information Figure S2).

Gold nanoparticle samples with FITC modified peptides were prepared and after one hour of incubation were centrifuged (14800 rpm for 20 min) for the separation of the adsorbed from the free peptides which obviously remains in the solution around the gold nanoparticles. Supernatant solution were carefully removed from the samples and were stored in epedorfs, meanwhile the participated was redissolved in the same quantity of Milli Q water. The detection of the adsorbed peptides on the gold nanoparticles collected after the centrifugation was not possible because of a strong quenching of fluorescence intensity of fluorescein as long as FITC molecules were now very close to the gold surface. This quenching effect provides one more critical information that confirms the adsorption of the peptide on the gold nanoparticles surface. So, in order to overcome this problem the detection and quantitative identification of FITC had to be done indirectly. Fluorescence measurments were acquired to the supernatant solution to determine the quantity of the free peptides. In Figure 5 are presented fluorescence images of supernatant solution at three representive molecular ratios. Using the calibration curve the exact amount of non adsorbed peptide was calculated for each one of the different samples. Taking into account the initial peptide concentration added on the gold nanoparticles solution, the amount of bounded peptides each time was calculated by subtraction. These values are presented in the Table S1 (Supporting Information).

The absolute value of the adsorbed peptides shows that the peptide concentration on the gold nanoparticles increases continuously. More specific, there was an increasing way of the adsorbed peptide concentration until the ratio of 450 but then this way decreases dramatically with the ratio. The best way to present these results is by the ratio of adsorbed to nonadsorbed peptides by the increasing peptide concentration (ratio of

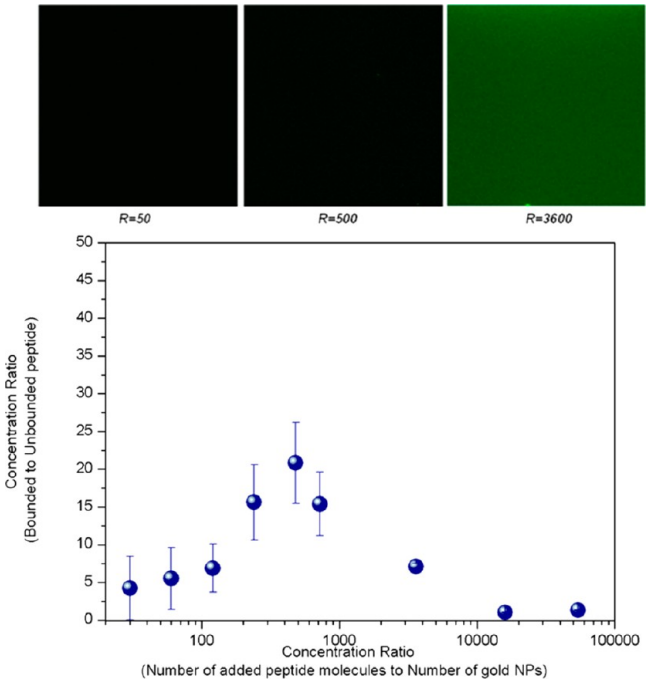

Figure 5. Images peptide functionalized gold nanoparticles in different peptide to gold ratios (top) and the ratio of bounded to unbounded peptides at different peptide loading calculated with fluorescence spectroscopy (down).

number of peptides to number of gold nanoparticles). These values are presented in Table S1 (Supporting Information).

In Figure 5 are presented the ratio of adsorbed to nonadsorbed peptides by the peptide concentration. More specific, it is very clear that there is an increase of the ratio of adsorbed peptides at low peptide loading until the ratio became around 450 but then, at higher peptide loading, this ratio decreases. Important information derives from these results. First of all, the peptides adsorbed easily on gold nanoparticles when these are isolated with large surface available because, as already mentioned,[61] of hydrophobic interactions. The adsorption rate in low peptide concentration consistently is high as long as the gold nanoparticles are not aggregated (free and almost isolated). The increase of the adsorption rate until the peptide ratio of around 500 might be caused to additional peptide−peptide.[61] As the peptide to gold NPs ratio becomes big enough the peptide−peptide interactions occurred among peptides, which are already adsorbed on neighbor gold nanoparticles. This is the main factor that leads to the aggregation of the peptide functionalized gold nanoparticles. Depletion forces between gold particles can be also important for considerable particle−particle interactions which additionally support this aggregation. This aggregation results in a decrease in the free surface where the peptides can be adsorbed. At higher peptide concentration, with ratio's more than 500, the adsorption rate decreases by increasing the concentration ratio (Figure 5). The pick on the Figure 5 corresponds to the conditions where aggregates start to be significant. This comes in correlation to the previous results from UV−vis spectroscopy and TEM, which proves that the aggregation occurs from the ratio of 250 to 500.

As result, a new material based on peptides adsorption via hydrophobic interactions on gold nanoparticles has been proposed. These hydrophobic interactions possess the

opportunity of reversible self-assembly gold nanoparticles as recently reported in the literature for PS-coated gold nanoparticles by Liz-Marzan et al.[62] However, in our case, the peptide functionalized gold nanoparticle aggregates are held together by hydrophobic gold−peptide and peptide−peptide interactions. It is also proved that there is a higher peptide affinity[61] to gold than to the other peptides. When gold nanoparticles were added to already formed aggregates, peptides prefer to be adsorbed on gold rather than to other peptides leading to a gradual disaggregation of the assemblies. Finally, if the added gold NPs were enough, single nanoparticles decorated with peptides can be formed. This mechanism describes the reversible self-assembly of AuΦ3 peptide functionalized gold nanoparticles. The advantage of peptide functionalization consists on the capability on easy and specific conjugation of peptide for a big variety of applications.

This material possesses two important characteristics that make it promising with a broad spectrum of applications. First of all, by adjusting the peptide concentration single gold nanoparticles decorated with peptides can be created, which make them usable for sensing, targeting and delivering of biological information. Second, bigger peptide concentrations bring to gold aggregates which are also preferably adjusted and can be used not only for biological applications, but also for more "smart" applications such as controlled drug release, controlled drug delivery etc. It can also be exploited the plasmon characteristics of gold nanoparticles which now can be tuned by the concentration of added peptides and used as an optical sensor or even more for the creation of SERS active substrates.

More detailed, higher peptide concentration was used for gold colloid aggregation in order to form SERS active substrates. Three, different samples were prepared to check possible formation of SERS active substrates by adding high AuΦ3 peptide concentration in 20 nm gold nanoparticles. The first sample was 200 μL of gold nanoparticles-AuΦ3 peptide at high molecular ratio (R = 1200) with 200 μL of 1 μg/mL adenine solution, the second was just 200 μL of gold nanoparticles-AuΦ3 peptide at high molecular ratio (R = 1200) and the third was 200 μL of gold nanoparticles with 200 μL of the same adenine solution. After the sample preparation, the solutions were placed under the Raman microscope in PS well-plate. In Figure 6 are presented the spectra collected from these different samples. It can be easily observed that second (gold nanoparticles with AuΦ3 peptide) and third (gold nanoparticles with 1 μg/mL adenine solution) sample, do not generate any significant Raman spectra. However, when spectra were acquired from the first sample (gold nanoparticles-AuΦ3 peptide at high molecular ratio with 1 μg/mL adenine solution) the characteristic Raman bands of adenine spectra were detected. This big enhancement in adenine's Raman spectra is due to the presence of aggregated gold nanoparticles. This phenomenon is well-known as surface enhanced Raman spectroscopy (SERS), and it is based on two enhancement mechanisms, the electromagnetic and the chemical,[63] which can enhance the Raman spectra even more than 12 orders of magnitudes. The chemical enhancement contributes a factor of 10^2 and the electromagnetic contributes dominantly with enhancement factors up to10^{12}. In our case, the SERS enhancement is mainly due to the electromagnetic enhancement. The gold aggregates create hot spots (points with very high generated electromagnetic field) mainly at the space between the aggregated particles. The plasmon coupling of gold

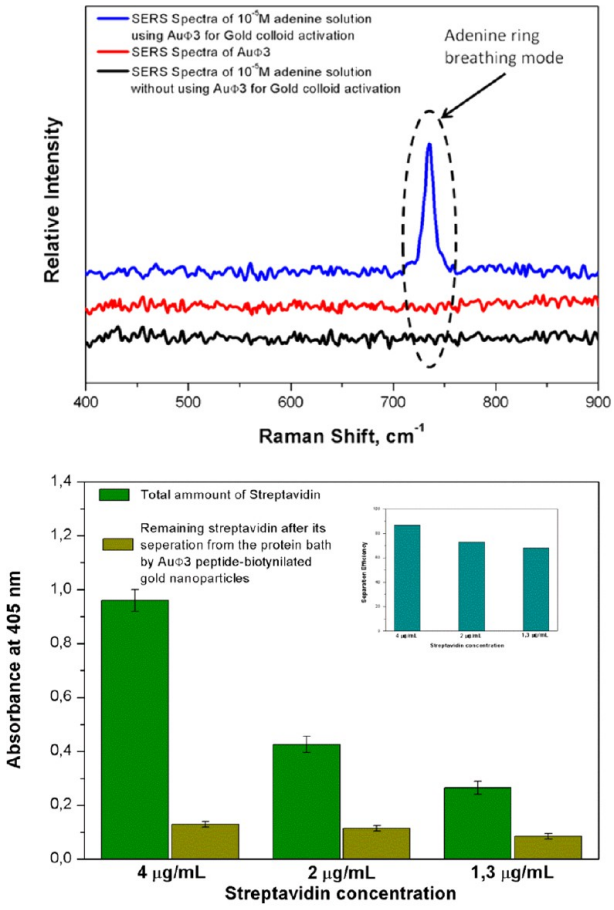

Figure 6. SERS spectra of adenine using AuΦ3 peptide for the gold nanoparticles aggregation−activation (top) and ELISA tests confirming the separation efficiency of the streptavidin from AuΦ3-biotinylated gold nanoparticles (bottom).

nanospheres in these hot spots produces very intense electromagnetic field and consequently strong SERS signals for the 780 nm laser line we have used for the experiments. For our set up the enhancement factor was estimated to10^5.

From the other side, single decorated gold nanoparticles were used as a separation-fishing technique. More specific, 500 μL of gold nanoparticles were incubating with low concentration of AuΦ3-biotinylated (single decorated gold nanoparticles) at room temperature for 1 h. For removal of peptide excess, peptide functionalized gold nanoparticles were centrifuged at 14 000 rpm on an eppendorf centrifuge for 10 min and rinsed several times. The gold-peptide pellet was separated from supernatant and redissolved in 500 μL of deionized water. This single decorated gold nanoparticle with AuΦ3-biotinylated was added in a bath of low concentration of BSA (bovine serum albumin) and streptavidin and incubated for 30 min at 37 °C. The sample was centrifuged at 14 000 rpm on an eppendorf centrifuge for 20 min. The supernatant solution was collected for the investigation of remaining streptavidin in the protein bath. Finally ELISA was developed by adding p-nitrophenyl phosphate substrate, verifying the successful separation of streptavidin from the aforementioned protein bath. In Figure 6, the medium absorbance at 405 nm is presented. This values represents the quantity of streptavidin in the bath before and after the separation with AuΦ3-biotinylated peptide functionalized gold nanoparticles with the separation efficiency on each

case (inset). These results come from of 10 different measurments, with the error bars, at three different streptavidin concentration protein baths.

CONCLUSIONS

In conclusion, this work demonstrates for the first time that AuΦ3 peptide adsorbs on 20 nm gold nanoparticles in a reversible and controlled fashion. By adjusting the ratio between the number of peptide molecules to number of gold nanoparticles, single gold nanoparticles decorated with AuΦ3 peptide as well as big gold aggregates can be formed. Fluorescence spectroscopy and ζ-potential measurments verified the adsorption of AuΦ3 peptide on gold nanoparticles and determined the exact amount of AuΦ3. The different gold nanoparticles structures upon the addition of AuΦ3 peptide has been investigated either spectroscopically with UV−vis absorption spectroscopy either by imaging with transmission electron microscopy. It is also important to note that such peptide-mediated gold structures are reversible by simply tuning the ratio between numbers of peptide molecules to number of gold nanoparticles as proved with UV−vis absorption spectroscopy. Finally, this new proposed nanomaterial has been used in two representive applications, one for gold aggregates for the generation of SERS active substrates and another for the single AuΦ3-peptide decorated gold nanoparticles with for streptavidin separation from proteins mixture.

ASSOCIATED CONTENT

Supporting Information

Gold nanoparticles UV−vis absorption spectrum and transmission electron microscopy, and AuΦ3 peptide UV−vis absorption spectrum presented in Figure S1, a calibration curve of AuΦ3-FITC with fluorescence spectroscopy presented in Figure S2, and the Table S1, which shows the values of added and adsorbed AuΦ3 upon different peptide loading using fluorescence spectroscopy. This material is available free of charge via the Internet at http://pubs.acs.org

AUTHOR INFORMATION

Corresponding Author

*E-mail: causa@unina.it.

Notes

The authors declare no competing financial interest.

ACKNOWLEDGMENTS

Authors would like to thank for their assistance Fabio Formiggini for the Fluorescence micro spectroscopy measurments, Valentina Mollo for the TEM images and Chiara Cosenza for the graphical support.

REFERENCES

(1) Nam, J. M.; Thaxton, C. S.; Mirkin, C. A. *Science* **2003**, *301*, 1884−1886.
(2) Seker, F.; Malenfant, P. R. L.; Larsen, M.; Alizadeh, A.; Conway, K.; Kulkarni, A. M.; Goddard, G.; Garaas, R. *Adv. Mater.* **2005**, *17*, 1941−1945.
(3) Reece, P. J. *Nat. Photonics* **2008**, *2*, 333−334.
(4) Boisselier, E.; Astruc, D. *Chem. Soc. Rev.* **2009**, *38*, 1759−1782.
(5) Daniel, M. C.; Astruc, D. *Chem. Rev.* **2004**, *104*, 293−346.
(6) Haick, H. *J. Phys. D: Appl. Phys* **2007**, *40*, 7173−7186.
(7) Zayats, M.; Baron, R.; Popov, I.; Willner, I. *Nano Lett.* **2005**, *5*, 21−25.
(8) Zhao, W.; Brook, M. A.; Li, Y. F. *ChemBioChem* **2008**, *9*, 2363−2371.
(9) Sperling, R. A.; Rivera Gil, P.; Zhang, F.; Zanella, M.; Parak, W. *Chem. Soc. Rev.* **2008**, *37*, 1896−1908.
(10) Radwan, S. H.; Azzazy, H. M. E *Expert Rev. Mol. Diagn.* **2009**, *9*, 511−524.
(11) Zeng, S. W.; Yong, K. T.; Roy, I.; Dinh, X. Q.; Yu, X.; Luan, F. *Plasmonics* **2011**, *6*, 491−506.
(12) Han, G.; Ghosh, P.; De, M.; Rotello, V. M.. *Nanobiotechnology* **2007**, *3*, 40−45.
(13) Sharma, P.; Brown, S.; Walter, G.; Santra, S.; Moudgil, B. *Adv. Colloid Interface Sci.* **2006**, *123−126*, 471−485.
(14) Glomm, W. R. *J. Dispersion Sci. Technol.* **2005**, *26*, 389−414.
(15) Taladriz-Blanco, P.; Buurma, N. J.; Rodriguez-Lorenzo, L.; Perez-Juste, J.; Liz-Marzan, L. M.; Herves, P. *J. Mater Chem.* **2011**, *21*, 16880−16887.
(16) Maye, M. M.; Lim, I-I. S.; Luo, J.; Rab, Z.; Rabinovich, D.; Liu, T.; Zhong, C.-J. *J. Am. Chem. Soc.* **2005**, *127*, 1519−1529.
(17) Wilson, R.; Chen, Y.; Aveyard, J. *Chem. Commun.* **2004**, 1156−1157.
(18) Bartz, M.; Kuther, J.; Nelles, G.; Weber, N.; Seshadri, R.; Tremel, W. *J. Mater. Chem.* **1999**, *9*, 1121−1125.
(19) Kanaras, A. G.; Kamounah, F. S.; Schaumburg, K.; Kiley, C.; Brust, M. *Chem. Commun.* **2002**, *20*, 2294−2295.
(20) Tshikhudo, T. R.; Wang, Z.; Brust, M. *Mater. Sci. Technol.* **2004**, *20*, 980−984.
(21) Gao, X.; Tao, W.; Lu, W.; Zhang, Q.; Zhang, Y.; Jiang, X.; Fu, S.. *Biomaterials* **2006**, *27*, 3482−3490.
(22) Kommareddy, S.; Amiji, M. *Nanomedicine* **2007**, *3*, 32−42.
(23) Tracy, J. B.; Kalyuzhny, G.; Crowe, M. C.; Balasubramanian, R.; Choi, J.-P.; Murray, R. W. *J. Am. Chem. Soc.* **2007**, *129*, 6706−6707.
(24) Becker, C. F. W.; Marsac, Y.; Hazarika, P.; Moser, J.; Goody, R. S.; Niemeyer, C. M. *ChemBioChem* **2007**, *8*, 32−36.
(25) Kim, Y.-P.; Oh, E.; Oh, Y.-H.; Moon, D. W.; Lee, T. G.; Kim, H.-S. *Angew. Chem., Int. Ed.* **2007**, *46*, 6816−6819.
(26) Slocik, J. M.; Tam, F.; Halas, N. J.; Naik, N. N. *Nano Lett.* **2007**, *7*, 1054−1058.
(27) Si, S.; Mandal, T. K. *Langmuir* **2007**, *23*, 190−195.
(28) Higuchi, M.; Ushiba, K.; Kawaguchi, M. *J. Colloid Interface Sci.* **2007**, *308*, 356−363.
(29) Tkachenko, A. G.; Xie, H.; Liu, Y.; Coleman, D.; Ryan, J.; Glomm, W. R.; Shipton, M. K.; Franzen, S.; Feldheim, D. L. *Bioconjugate Chem.* **2004**, *15*, 482−490.
(30) Oyelere, A. K.; Chen, P. C.; Huang, X.; El-Sayed, I. H.; El-Sayed, A. M. *Bioconjugate Chem.* **2007**, *18*, 1490−1497.
(31) Pengo, P.; Baltzer, L.; Pasquato, L.; Scrimin, P. *Angew. Chem., Int. Ed.* **2007**, *46*, 400−404.
(32) Fillon, Y.; Verma, A.; Ghosh, P.; Ernenwein, D.; Rotello, V. M.; Chmielewski, J. *J. Am. Chem. Soc.* **2007**, *129*, 6676−6677.
(33) Satyabrata, S.; Manoj, R.; Tapas, K. P.; Tarun, K. M. *ChemPhysChem* **2008**, *9*, 1578−1584.
(34) Levy, R.; Thanh, N. T. K.; Doty, R. C.; Hussain, I.; Nichols, R. J.; Schiffrin, D. J.; Brust, M.; Fernig, D. G. *J. Am. Chem. Soc.* **2004**, *126*, 10076−10084.
(35) Levy, R. *ChemBioChem* **2006**, *7*, 1141−1145.
(36) Brennan, J. L.; Hatzakis, N. S.; Tshikhudo, T. R.; Dirvianskyte, N.; Razumas, V.; Patkar, S.; Vind, J.; Svendsen, A.; Nolte, R. J. M.; Rowan, A. E.; Brust, M. *Bioconjugate Chem.* **2006**, *17*, 1373−1375.
(37) Park, J.-A.; Lee, J.-J.; Kim, I.-S.; Park, B.-H.; Lee, G.-H.; Kim, T.-J.; Ri, H.-C.; Kim, H.-J.; Chang, Y. *Colloids Surf., A* **2008**, *31*, 288−291.
(38) Prosperi, D.; Morasso, C.; Tortora, P.; Monti, D.; Bellini, T. *ChemBioChem* **2007**, *8*, 1021−1028.
(39) Weiss, B.; Schneider, M.; Muys, L.; Taetz, S.; Neumann, D.; Schaefer, U. F.; Lehr, C.-M. *Bioconjugate Chem.* **2007**, *18*, 1087−1094.
(40) Ackerson, C. J.; Jadzinsky, P. D.; Jensen, G.-J.; Kornberg, R. D. *J. Am. Chem. Soc.* **2006**, *128*, 2635−2640.
(41) You, C.-C.; Verma, A.; Rotello, V. M. *Soft Mater.* **2006**, *2*, 190−204.

(42) Shang, L.; Wang, Y.; Jiang, J.; Dong, S. *Langmuir* **2007**, *23*, 2714−2721.
(43) Schroedter, A.; Weller, H. *Angew. Chem., Int. Ed* **2002**, *41*, 3218−3221.
(44) Zhang, S. G. *Nat. Biotechnol.* **2003**, *21*, 1171−1178.
(45) Sarikaya, M.; Tamerler, C.; Jen, A. K. Y.; Schulten, K.; Baneyx, F. *Nat. Mater.* **2003**, *2*, 577−585.
(46) Hersel, U.; Dahmen, C.; Kessler, H. *Biomaterials* **2003**, *24*, 4385−4415.
(47) Hamley, I. W. *Angew. Chem.* **2007**, *119*, 8128−8147.
(48) Ulijn, R. V.; Smith, A. M. *Chem. Soc. Rev.* **2008**, *37*, 664−675.
(49) Mart, R. J.; Osborne, R. D.; Stevens, M. M.; Ulijn, R. V. *Soft Matter* **2006**, *2*, 822−835.
(50) Shin, H.; Jo, S.; Mikos, A. G. *Biomaterials* **2003**, *24*, 4353−4364.
(51) Lutolf, M. P.; Hubbell, J. A. *Nat. Biotechnol.* **2005**, *23*, 47−55.
(52) Ellis-Behnke, R. G.; Liang, Y.-X.; David, K. C.; Kau, P.W. F.; Schneider, G. E.; Zhang, S.; Wu, W.; So, K.-F. *Nanomedicine* **2006**, *2*, 207−215.
(53) Porta, F.; Speranza, G.; Krpetic, Z.; Dal Santo, V.; Francescato, P.; Scari, G. *Mater. Sci. Eng., B.* **2007**, *140*, 187−194.
(54) Brown, S. *Nat. Biotechnol.* **1997**, *15*, 269−272.
(55) Segvich, S. J.; Smith, H. C.; Kohn, D. H. *Biomaterials* **2009**, *30*, 1287−1298.
(56) Naik, R. R.; Stringer, S. J.; Agarwal, G.; Jones, S. E.; Stone, M. O. *Nat. Mater.* **2002**, *1*, 169−172.
(57) Slocik, J. M.; Stone, M. O.; Naik, R. R. *Small* **2005**, *1*, 1048−1052.
(58) Kim, J.; Sadowsky, M. J.; Hur, H.-G. *Biomacromolecules* **2011**, *12*, 2518−2523.
(59) Polavarapu, L.; Xu, Q.-H. *Langmuir* **2008**, *24*, 10608−10611.
(60) Slocik, J. M.; Zabinsky, J. S.; Phillips, D. M.; Naik, R. R. *Small* **2008**, *4*, 548−551.
(61) Causa, F.; Della Moglie, R.; Iaccino, E.; Mimmi, S.; Marasco, D.; Scognamiglio, P. L.; Battista, E.; Palmieri, C.; Cosenza, C.; Sanguigno, L.; Quinto, I.; Scala, G.; Netti, P. A. *J. Colloid Interface Sci.* **2012**, *389*, 220−229.
(62) Sanchez-Iglesias, A.; Grzelczak, M.; Altantzis, T.; Goris, B.; Perez-Juste, J.; Bals, S.; Van Tendeloo, G.; Donaldson, S. H.; Chmelka, B. F.; Israelachvili, J. N.; Liz-Marzan, L. M. *ACS Nano* **2012**, *6*, 11059−11065.
(63) Kneipp, K.; Kneipp, H.; Itzkan, I.; Dasari, R. R.; Feld, M. S. *Chem. Rev.* **1999**, *99*, 2957−2976.